A Kalman Filter based Predictive Direct Power Control Scheme to Mitigate Source Voltage Distortions in PWM Rectifiers

Un-chul Moon[*], Soo-eon Kim[*], Roh Chan[*], and Sangshin Kwak[†]

[*,†]School of Electrical and Electronics Engineering, Chung-ang University, Seoul, Korea

Abstract

In this paper, a predictive direct power control (DPC) method based on a Kalman filter is presented for three-phase pulse-width modulation (PWM) rectifiers to improve the performance of rectifiers with source voltages that are distorted with harmonic components. This method can eliminate the most significant harmonic components of the source voltage using a Kalman filter algorithm. In the process of predicting the future real and reactive power to select an optimal voltage vector in the predictive DPC, the proposed method utilizes source voltages filtered by a Kalman filter, which can mitigate the adverse effects of distorted source voltages on control performance. As a result, the quality of the source currents synthesized using the PWM rectifier is improved, and the total harmonic distortion (THD) values are reduced, even under distorted source voltages.

Key words: Three-phase pulse-width modulated rectifier, Direct power control, Predictive control, Kalman filter

I. INTRODUCTION

Diode rectifiers and thyristor rectifiers for AC-to-DC conversion can cause problems in power transmission and distribution lines due to distorted source currents and voltages. In addition, the ripple components in the DC-link voltage in diode rectifiers and thyristor rectifiers are also high [1]. With the aim of satisfying the IEEE 519 standards and IEC 61000 regulations for power line quality, three-phase pulse-width modulation (PWM) rectifiers can reduce the distortion in power lines with sinusoidal input currents. Furthermore, the low ripple components of the DC-link voltage, controllable power factor, and regeneration capability can be achieved using PWM rectifiers [4]-[6]. Control methods for PWM rectifiers can be classified into two groups: oriented control (OC) and direct power control (DPC). The OC methods use current control loops, whereas the DPC methods utilize power control loops [7]. The OC methods for PWM rectifiers can be categorized based on the control algorithm. They are voltage oriented control (VOC) [8]-[10] and virtual flux

oriented control (VFOC) [9], [11]-[13]. The algorithms based on the supply voltage and the virtual flux of the supply voltage are regarded as VOC and VFOC, respectively. Likewise, the DPC methods can be classified as Voltage based Direct Power Control (V-DPC) [14], [15] and Virtual Flux based Direct Power Control (VF-DPC) [16]. Hysteresis controllers and switching tables have been used to control the PWM rectifiers in the conventional oriented control and DPC methods [9], [14]. In addition to hysteresis controllers, the oriented control and DPC methods based on space vector modulation (SVM) have been developed [7], [17], [18]. Recently, with the development of fast microprocessors, predictive control methods have been presented as simple and effective control methods for various power converters including PWM rectifiers, which do not need individual PWM blocks, and the design of control loops for regulating PI gains and obtaining small signal models [19]. The predictive direct power control methods for PWM rectifiers are based on predicting future real and reactive power components to select an optimal voltage vector, which are in turn calculated by the source voltages. Therefore, distorted source voltages of PWM rectifiers result in deteriorated performance of PWM rectifiers, such as increased harmonic distortions of the input currents and increased ripples in the power components [7], [20].
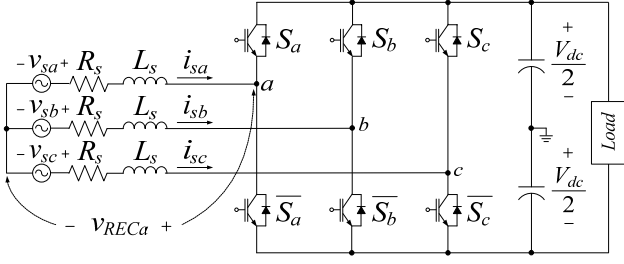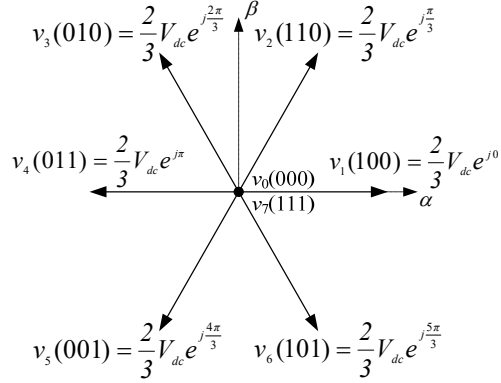
Fig. 1. Three-phase active rectifier.

Fig. 2. Voltage vectors of the PWM rectifier.

With these factors in mind, a predictive direct power control method based on a Kalman filter is proposed in this paper for three-phase pulsewidth modulation (PWM) rectifiers to improve the performance of rectifiers with source voltages distorted with harmonic components. This method eliminates the most significant harmonic components of source voltage on the basis of a Kalman filter algorithm. In the process of predicting the future real and reactive power to select an optimal voltage vector in the predictive direct power control method, the proposed method utilizes source voltages filtered by a Kalman filter, which can mitigate the adverse effects of distorted source voltages on control performance. As a result, the quality of the source currents synthesized by the PWM rectifier are improved with a reduced total harmonic distortion value (THD), even under distorted source voltages. Simulation and experimental results are presented to verify the proposed method based on a Kalman filter algorithm.

II. MODEL PREDICTIVE DIRECT POWER CONTROL METHOD FOR THREE-PHASE PWM RECTIFIERS

The predictive direct power control method directly adjusts the input active and reactive power by predicting the future input powers based on a mathematical model of a three-phase PWM rectifier. A three-phase PWM rectifier with six switches, connected to a three-phase voltage source through the input filter inductances L_s and resistances R_s at its input side, is shown in Fig. 1. The upper switches consist of S_a, S_b, and S_c while the upper and the lower switches of the active rectifier are complementarily operated. For the mathematical

model of the PWM rectifier, the source voltage vector, input current vector, and rectifier input voltage vector are defined as:

$$\begin{aligned} \boldsymbol{v}_s &= \begin{bmatrix} v_{sa} & v_{sb} & v_{sc} \end{bmatrix}^{\mathrm{T}} \\ \boldsymbol{i}_s &= \begin{bmatrix} i_{sa} & i_{sb} & i_{sc} \end{bmatrix}^{\mathrm{T}} \\ \boldsymbol{v}_{REC} &= \begin{bmatrix} v_{RECa} & v_{RECb} & v_{RECc} \end{bmatrix}^{\mathrm{T}} \end{aligned} \quad (1)$$

where, $\boldsymbol{v}_s$ is the three-phase source voltage vector, $\boldsymbol{i}_s$ is the input current vector, and $\boldsymbol{v}_{REC}$ is the input voltage generated by the PWM rectifier. On the basis of (2), these vectors can be expressed in the vector forms of the $\alpha\beta$ orthogonal coordinates.

$$\begin{bmatrix} x_\alpha \\ x_\beta \end{bmatrix} = \frac{2}{3} \begin{bmatrix} 1 & -\frac{1}{2} & -\frac{1}{2} \\ 0 & \frac{\sqrt{3}}{2} & -\frac{\sqrt{3}}{2} \end{bmatrix} \begin{bmatrix} x_a \\ x_b \\ x_c \end{bmatrix} \quad (2)$$

The PWM rectifier can produce eight voltage vectors, $\boldsymbol{v}_{REC}$, as shown in Fig. 2, including six active and two zero vectors. These vectors depend on the switching states of the three upper switches, S_a, S_b, and S_c. By selecting the optimal voltage vector among the eight voltage vectors at every sampling period, the PWM rectifier can regulate the dc-link voltage as well as control the active and reactive power, leading to sinusoidal input current synthesis. The input current dynamics of the PWM rectifier are obtained in the continuous-time model as:

$$L_s \frac{d\boldsymbol{i}_s}{dt} = \boldsymbol{v}_s - \boldsymbol{v}_{REC} - R\boldsymbol{i}_s \quad (3)$$

By using an Euler approximation with a sampling period of T_s in (3), the input current at the $(k + 1)$th instant can be represented in the discrete-time domain as [19]:

$$\boldsymbol{i}_s(k+1) = \left(1 - \frac{R_s T_s}{L_s}\right)\boldsymbol{i}_s(k) + \frac{T_s}{L_s}\left[\boldsymbol{v}_s(k) - \boldsymbol{v}_{REC}(k)\right]. \quad (4)$$

At the kth instant, the one-step future input current vector $\boldsymbol{i}_s(k + 1)$ required in (5) can be calculated with the measured input current vector $\boldsymbol{i}_s(k)$, the measured source voltage vector $\boldsymbol{v}_s(k)$ and the presently applied PWM rectifier input voltage vector $\boldsymbol{v}_{REC}(k)$. A delay compensation scheme is included to alleviate the control delay caused by the calculation time in the controller. By shifting the input current at the $(k + 1)$th instant in (4) one step forward to employ the delay compensation scheme, the future input current at the $(k + 2)$th instant is expressed as [19]:

$$\boldsymbol{i}_s(k+2) = \left(1 - \frac{R_s T_s}{L_s}\right)\boldsymbol{i}_s(k+1) + \frac{T_s}{L_s}\left[\boldsymbol{v}_s(k+1) - \boldsymbol{v}_{REC}(k+1)\right] \quad (5)$$

In addition, the future source voltage $\boldsymbol{v}_s(k + 1)$ required in (5) can be calculated with:

$$\boldsymbol{v}_s(k+1) = \boldsymbol{v}_s(k)e^{j\Delta\theta} \quad . \quad (6)$$

where, the angle variation of the source voltage vector with its angular frequency ω in one sampling period, $\Delta\theta$, is equal to ωT_{sp}. Thus, the eight future input current vectors $\boldsymbol{i}_s(k + 2)$ at the $(k + 2)$th instant can be predicted in accordance with

the eight rectifier input voltage vectors, $v_{REC}(k + 1)$ using (5). In the predictive DPC method for the PWM rectifier, the eight future instantaneous input powers at the $(k + 2)$th instant can be also predicted using the eight input currents predicted in (5) as:

$$P(k+2) = \text{Re}\{v_s(k+2)\bar{i}_s(k+2)\} = v_{s\alpha}(k+2)i_{s\alpha}(k+2) + v_{s\beta}(k+2)i_{s\beta}(k+2)$$
(7)

$$Q(k+2) = \text{Im}\{v_s(k+2)\bar{i}_s(k+2)\} = v_{s\beta}(k+2)i_{s\alpha}(k+2) - v_{s\alpha}(k+2)i_{s\beta}(k+2)$$
(8)

where, $i_{s\alpha}(k + 2)$, $i_{s\beta}(k + 2)$, $v_{s\alpha}(k + 2)$, and $v_{s\beta}(k + 2)$ are the predicted future input currents and calculated future source voltages at the $(k + 2)$th instant in the $\alpha\beta$ frame. The future source voltage $v_s(k + 2)$ at the $(k + 2)$th instant required in (7) and (8) can be calculated by reapplying (6). Among the eight possible switching states that produce the eight future instantaneous input real and reactive powers at the $(k + 2)$th instant, one optimal switching state corresponding to the optimal rectifier input voltage vector, $v_{REC}(k + 1)$, is selected to minimize the input power error based on a cost function defined as:

$$g = \left| P^* - P(k+2) \right| + \left| Q^* - Q(k+2) \right|$$
(9)

In the predictive DPC algorithm for PWM rectifiers, the reference real power P^* in (9) can be obtained as the output of the PI controller used to regulate the DC-link voltage. On the other hand, the reference reactive power Q^* is generally set to zero to produce sinusoidal input currents that are in phase with the source voltage.

III. Proposed Source Voltage Harmonic Reduction Technique for the Predictive DPC Method based on a Kalman Filter

Disturbances in the source voltage have adverse effects on the input currents as well as the input real and reactive power control in the PWM rectifier. As a result, it is desirable to eliminate the harmonic components of the source voltage to improve the PWM rectifier performance. The proposed method develops a source voltage harmonic reduction technique in the predictive DPC for PWM rectifiers, using a Kalman filter, to prevent the detrimental effects of harmonics and noise in the source voltage on the PWM rectifier performance. Using the proposed method, the PWM rectifier can provide sinusoidal input current synthesis and accurate input power control, even under a distorted source voltage with harmonic components. A standard Kalman filter algorithm can be expressed as [21]:

$$x(k+1) = Ax(k) + Bu(k) + w(k)$$

$$z(k) = Hx(k) + n(k)$$
(10)

where, x is a state vector, u is a control input, A and B are constant matrices, w is process noise, z is an output, H is an output matrix, n is a measurement noise, and k is a discrete time index, respectively. The two noise variables, w and v, are assumed to be independent white noises with normal distributions with covariance of Q and R, respectively. In this paper, the standard Kalman filter algorithm is applied to track the fundamental frequency component from the source voltage v_s, which is distorted with harmonic components and noises. The Kalman filter is a kind of state observer which tracks the state form measurement output based on stochastic information of noise. Therefore, the Kalman filter can be used to extract the fundamental harmonic component from v_s, because the measured source voltage v_s contains high-order harmonics. In this system, the output variable z can be changed with the source voltage v_s, and there is no control input u for v_s. Thus, the discrete time model in (10) can be changed to:

$$x(k+1) = Ax(k) + w(k)$$

$$v_s(k) = Hx(k) + n(k)$$
(11)

The a priori estimate of the state $\hat{x}^-(k)$ and the a priori estimate of the error covariance $P^-(k)$ under k-th discrete time step are calculated as [21]:

$$\hat{x}^-(k) = A\hat{x}(k-1)$$
(12)

$$P^-(k) = AP(k-1)A^T + Q$$
(13)

Then, the Kalman gain K, the state estimate $\hat{x}$, and the error covariance P are updated at every sampling step to allow for the calculation of the state estimate as:

$$K(k) = P^-(k)H^T\{HP^-(k)H^T + R\}^{-1}$$
(14)

$$\hat{x}(k) = \hat{x}^-(k) + K(k)\{y(k) - H\hat{x}^-(k)\}$$
(15)

$$P(k) = P^-(k) - K(k)HP^-(k)$$
(16)

Therefore, $\hat{x}$ in (14) represent an estimate of the real state x using the Kalman filter algorithm. In this paper, to apply the Kalman filter algorithm to a source voltage with harmonic components, the measured source voltage v_s with high-order harmonics is represented as:

$$v_s = \sum y_i = y_1 + y_2 + y_3 + \cdots + n$$
(17)

where, y_1 is the fundamental component of the source voltage, $y_i (i = 2,3,\ldots)$ is the i-th harmonic component contained in the source voltage, and n is the measurement noise. Assuming that the fundamental frequency of the source voltage is 60 Hz, the angular frequency of y_i, ω_i, is expressed as $120\pi i$. For a sinusoidal solution to the second order dynamic equation, each i-th component, y_i, can be represented as a solution of:

$$\ddot{y}_i + \omega_i^2 y_i = 0.$$
(18)

By defining $x_1 = y_i$, $x_2 = \dot{y}_i$, the state equation of y_i can be written as:

$$\begin{bmatrix} \dot{x}_1 \\ \dot{x}_2 \end{bmatrix} = \begin{bmatrix} 0 & 1 \\ -\omega_i^2 & 0 \end{bmatrix} \begin{bmatrix} x_1 \\ x_2 \end{bmatrix}$$

$$y_i = \begin{bmatrix} 1 & 0 \end{bmatrix} \begin{bmatrix} x_1 \\ x_2 \end{bmatrix}$$
(19)

This implies that two state variables are required to

represent each harmonic component. Thus, the measured source voltage is represented by the standard continuous equation as:

$$\dot{x} = A_C x + w$$
$$v_s = Hx + n \,. \tag{20}$$

where, x, A_C, and H have dimensions of $(2m + 2) \times 1$, $(2m + 2) \times (2m + 2)$, and $1 \times (2m + 2)$, and the noises w and n have dimensions of $(2m + 2) \times 1$ and scalar, respectively. In addition, m is the number of harmonics contained in the source voltage that need to be considered. For example, the 5th and 7th harmonic components in the source voltage are considered, without loss of generality, the measured source voltage v_s is represented a sum of three components (the fundamental, the 5th harmonic, and the 7th harmonic components) as:

$$v_s = y_1 + y_5 + y_7 + n \tag{21}$$

With the definition of $x_1 = y_1$, $x_2 = \dot{y}_1$ $x_3 = y_5$, $x_4 = \dot{y}_5$, $x_5 = y_7$, and $x_6 = \dot{y}_7$, an equation considering the 5th and 7th harmonics in the source voltage can be represented in an augmented form as:

$$\dot{x} = \begin{bmatrix} \dot{x}_1 \\ \dot{x}_2 \\ \dot{x}_3 \\ \dot{x}_4 \\ \dot{x}_5 \\ \dot{x}_6 \end{bmatrix} = A_C x = \begin{bmatrix} 0 & 1 & 0 & 0 & 0 & 0 \\ -\omega_1^2 & 0 & 0 & 0 & 0 & 0 \\ 0 & 0 & 0 & 1 & 0 & 0 \\ 0 & 0 & -\omega_5^2 & 0 & 0 & 0 \\ 0 & 0 & 0 & 0 & 0 & 1 \\ 0 & 0 & 0 & 0 & -\omega_7^2 & 0 \end{bmatrix} \begin{bmatrix} x_1 \\ x_2 \\ x_3 \\ x_4 \\ x_5 \\ x_6 \end{bmatrix}$$

$$= \begin{bmatrix} 0 & 1 & 0 & 0 & 0 & 0 \\ -(120\pi)^2 & 0 & 0 & 0 & 0 & 0 \\ 0 & 0 & 0 & 1 & 0 & 0 \\ 0 & 0 & -(600\pi)^2 & 0 & 0 & 0 \\ 0 & 0 & 0 & 0 & 0 & 1 \\ 0 & 0 & 0 & 0 & -(720\pi)^2 & 0 \end{bmatrix} \begin{bmatrix} x_1 \\ x_2 \\ x_3 \\ x_4 \\ x_5 \\ x_6 \end{bmatrix}$$

$$v_s = Hx = \begin{bmatrix} 1 & 0 & 1 & 0 & 1 & 0 \end{bmatrix} \begin{bmatrix} x_1 \\ x_2 \\ x_3 \\ x_4 \\ x_5 \\ x_6 \end{bmatrix} \tag{22}$$

When only the 5th harmonic component is considered in the source voltage, the two states, x_5 and x_6, caused by the 7th harmonics can be removed using (22), which yields A_C and H, with reduced dimensions to 4×4 and 1×4, respectively. Thus, A_C becomes:

$$A_C = \begin{bmatrix} 0 & 1 & 0 & 0 \\ -\omega_1^2 & 0 & 0 & 0 \\ 0 & 0 & 0 & 1 \\ 0 & 0 & -\omega_2^2 & 0 \end{bmatrix} = \begin{bmatrix} 0 & 1 & 0 & 0 \\ -(120\pi)^2 & 0 & 0 & 0 \\ 0 & 0 & 0 & 1 \\ 0 & 0 & -(600\pi)^2 & 0 \end{bmatrix} \tag{23}$$

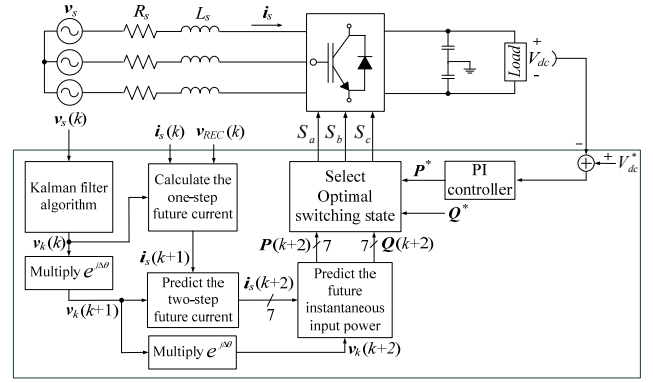To make the system take on a discrete form, the transition matrix A with the sampling time T_s is:

Fig. 3. Block diagram of the proposed method.

$$A = e^{A_C T_s} = \sum_{n=0}^{\infty} \frac{1}{n!} A_C^{\,n} T_s^{\,n} = I + A_C T_s + \frac{1}{2!} A_C^{\,2} T_s^{\,2} + \frac{1}{3!} A_C^{\,3} T_s^{\,3} + \cdots \tag{24}$$

Then, the voltage system can be represented in discrete form as (10). The discrete form with a sampling time of $T_s = 0.00005$ [s] can be written as:

$$\begin{bmatrix} x_1(k+1) \\ x_2(k+1) \\ x_3(k+1) \\ x_4(k+1) \end{bmatrix} = \begin{bmatrix} 0.9988 & 0 & 0 & 0 \\ -7.1057 & 0.9988 & 0 & 0 \\ 0 & 0 & 0.9956 & 0 \\ 0 & 0 & -177.39 & 0.9956 \end{bmatrix} \begin{bmatrix} x_1(k) \\ x_2(k) \\ x_3(k) \\ x_4(k) \end{bmatrix} + w(k)$$

$$v_s(k) = \begin{bmatrix} 1 & 0 & 1 & 0 \end{bmatrix} \begin{bmatrix} x_1(k) \\ x_2(k) \\ x_3(k) \\ x_4(k) \end{bmatrix} + n(k) \tag{25}$$

Thus, based on (11) to (15), the Kalman filter algorithm can be utilized to eliminate the harmonic components contained in the source voltage at every sampling period. The first output component of v_s, which corresponds to the state x_1, represents the pure fundamental component of v_s, without the 5th harmonic component and noises. The filtered source voltage with harmonic mitigation using the Kalman filter algorithm, $v_k(k)$, can be obtained using the measured source voltage, $v_k(k)$, at each sampling instant. In the proposed method, at the kth instant, the filtered source voltage, $v_k(k)$, instead of the measured source voltage, $i_s(k)$, is used to avoid the adverse effects caused by distortions of the source voltage. The input current at the $(k + 1)$th instant can be calculated using the measured input current vector, $i_s(k)$, the filtered source voltage, $i_s(k)$, and the presently applied active rectifier input voltage vector, $v_{REC}(k)$, determined at the $(k - 1)$th instant. Then, the eight future input current vectors and the instantaneous input real and reactive powers at the $(k + 2)$th instant are predicted using $v_k(k)$ in the same manner used in the conventional method. Among the eight possible switching states, the one optimal switching state corresponding to an optimal rectifier input voltage vector, $v_{REC}(k + 1)$, is then selected to minimize the input power error based on a cost function. Fig. 3 shows an overall block diagram of the proposed method.

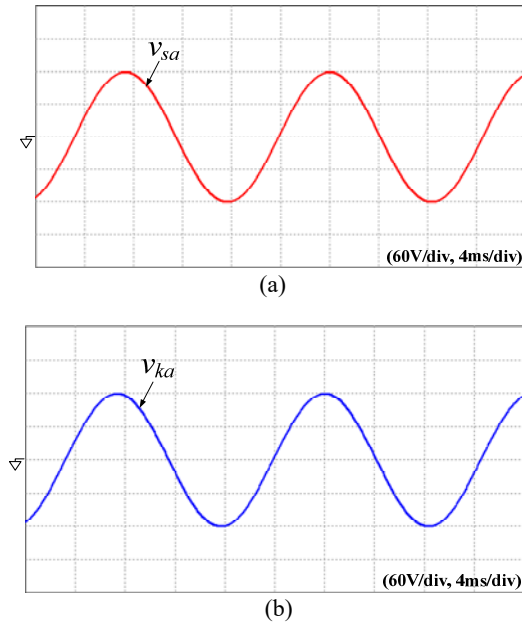**(60V/div, 4ms/div)**

(a)

(60V/div, 4ms/div)

(b)

Fig. 4. Simulation results of the measured and filtered source voltages in the case of no harmonic components in the source voltage at 120 V and 60 Hz: (a) measured source voltage and (b) voltage filtered using the proposed method based on the Kalman filter algorithm.

Fig. 5. Simulation results of the measured and filtered source voltages in the case that the *a*-phase source voltage contains the 5th harmonic component at 30% of the fundamental component: (a) measured source voltage and (b) voltage filtered using the proposed method based on the Kalman filter algorithm

IV. SIMULATION AND EXPERIMENT RESULTS

The proposed method, based on a Kalman filter algorithm to eliminate the harmonic components of source voltage, was simulated under the conditions of a peak value of the source voltage v_s= 120 V, R_s = 0.8 Ω, L_s = 16 mH, C = 1100 μF, V_{dc}^*= 260 V, R_{load} = 100 Ω, T_s = 50 μs. Fig. 4 shows simulated waveforms of the measured source voltage and the resultant source voltage obtained by the Kalman filter algorithm for the *a*-phase source voltage in the case of a source voltage with no harmonic contamination. The measured *a*-phase source voltage v_{sa}, is shown in Fig. 4(a). The voltage filtered by the Kalman filter v_{ka}, is shown in Fig. 4 (b). In the case with no harmonic components of the source voltage, the source voltage filtered using the proposed method based on a Kalman filter is very similar to the measured source voltage. The average error between the measured source voltage, v_{sa}, and the filtered voltage, v_{ka}, with 10,000 consecutive samples is defined as the average error between v_{sa} and v_{ka} with 10,000 sampled data points:

$$= \frac{\sum_{n=1}^{10,000} |v_{sa}(n) - v_{ka}(n)|}{10,000} \qquad (26)$$

In Fig. 4, the average error was 0.0566 V.

Fig. 5 illustrates simulation waveforms of the measured source voltage and the voltage filtered by the proposed method based on a Kalman filter in the case of an a-phase source voltage that contains the 5th harmonic component at 30% of the fundamental component. Fig. 5(b) shows that the
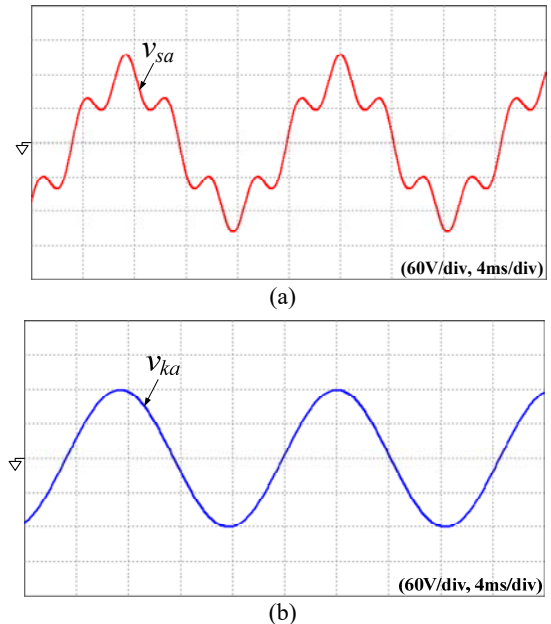
proposed method can filter out the 5th harmonic component of the source voltage. Using the filtered source voltage with the reduced harmonic components of the distorted source voltage, the proposed method shows improved performance in the predictive DPC method in terms of the total harmonic distortion (THD) of the input currents and the power error between the actual power and the power reference, when compared to the case without the Kalman filter.

For a distorted source voltage, as shown in Fig. 5(a), simulation waveforms obtained using the proposed predictive DPC method based on a Kalman filter are shown in Fig. 6. For comparison, the simulation results obtained without the Kalman filter are included in Fig. 6(a). This figure shows that the input current is distorted for the distorted source voltage without the Kalman filter. On the other hand, the proposed method based on a Kalman filter can lead to an improved input current waveform because of the filtering effect of the Kalman filter, as shown in Fig. 6(b) when compared with Fig. 6(a). The dynamic performance of the proposed method with a source voltage disturbance is shown in Fig. 7, with a step-change in the real power reference from 600 W to 1000 W and with the reactive power set to zero. As shown in Fig. 7, a fast dynamic response and no coupling between the real and reactive power components are obtained using the proposed method. The input current waveform from the proposed method is sinusoidal and has a low THD in the transient condition with a distorted source voltage, as shown in Fig. 7(b) [unlike the input current waveform obtained without a Kalman filter in Fig. 7(a)]. In addition, simulation results
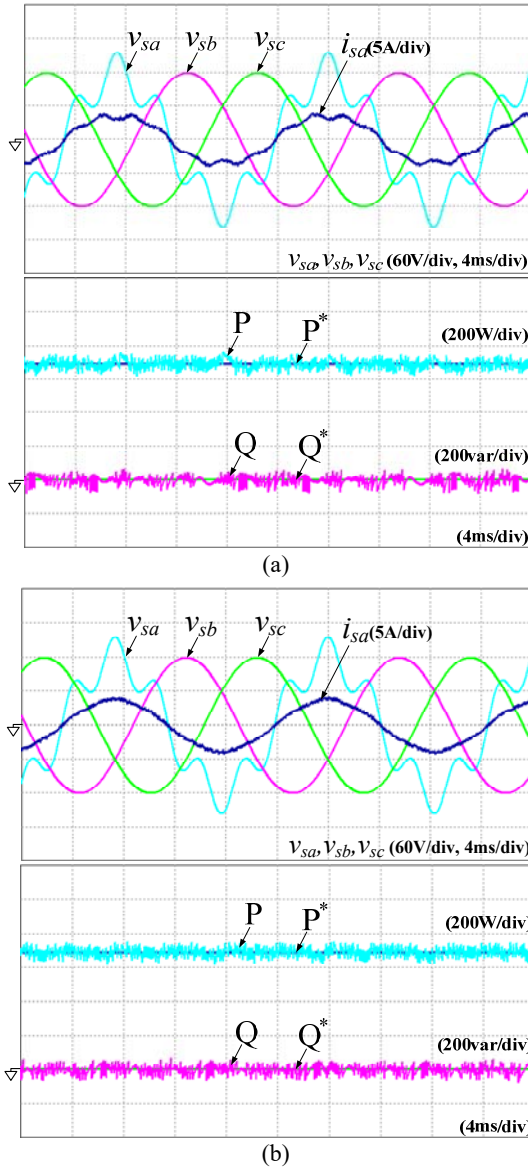
Fig. 6. Simulation results of the three-phase source voltages, the *a*-phase input current, the actual and the reference values of the real and reactive power in the case in which the *a*-phase source voltage contains the 5th harmonic component at 30% of the fundamental component with P* = 1000 W, Q* = 0, and T_s = 50 μs: (a) without the Kalman filter and (b) the proposed method based on the Kalman filter algorithm.
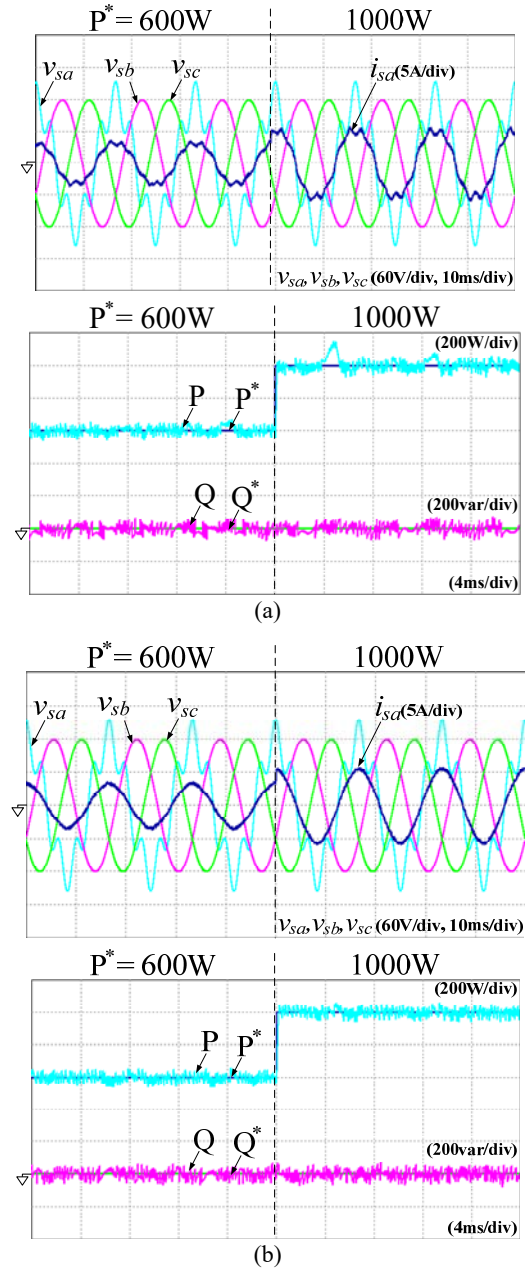

Fig. 7. Simulation results with the step-change of the real power reference from 600 W to 1000 W in the case of the *a*-phase source voltage disturbance: (a) without the Kalman filter and (b) the proposed method.

with a step-change of the reactive power reference from -200 var to 200 var, and results for a real power fixed at 600 W are shown in Fig. 8. Fig. 8(a) shows that a distorted input current waveform without a Kalman filter results from the distorted source voltage. As in the step-change in the real power reference, the proposed method leads to no coupling between the real and reactive power components and a fast dynamic response depending on a step-change of the reactive power reference with a distorted source voltage, as shown in the Fig. 8(b). Furthermore, the proposed method synthesizes a sinusoidal input current, despite the distorted source voltage waveform, whereas the phase difference between the source

voltage and the input currents changes depending on the change of the reactive power reference.

The proposed method utilizing the Kalman filter algorithm was tested with a prototype PWM rectifier setup. The setup consisted of a PWM rectifier with an IGBT module, a 16-mH input filter inductance, a 0.8Ω input resistance, and a 1100-µF DC-link capacitor. The peak value of the source voltage, the DC-link voltage reference, and the load resistance were set to 120 V, 260 V, and 100Ω, respectively. The proposed predictive DPC method based on a Kalman filter was implemented on a DSP board (TMS320F28335)
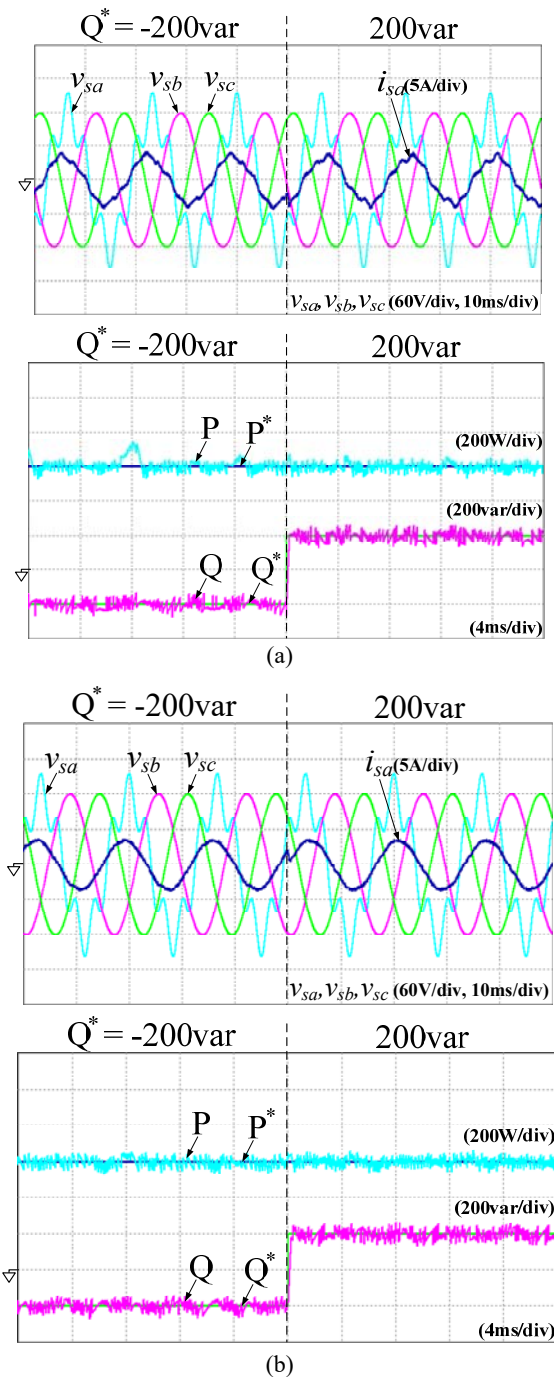
Fig. 8. Simulation results with the step-change of the reactive power reference from -200 var to 200 var in the case of *a*-phase source voltage disturbance: (a) without the Kalman filter and (b) the proposed method.

with $T_s = 50$ μs to generate sinusoidal input currents with a unity power factor. When the *a*-phase source voltage contains the 5th harmonic component that is 30% of the fundamental component, the experimental waveforms obtained by the proposed predictive direct power control method based on a Kalman filter are shown in Fig. 9 along with comparative experimental results obtained without a Kalman filter. It is seen that the input current is distorted with the distorted
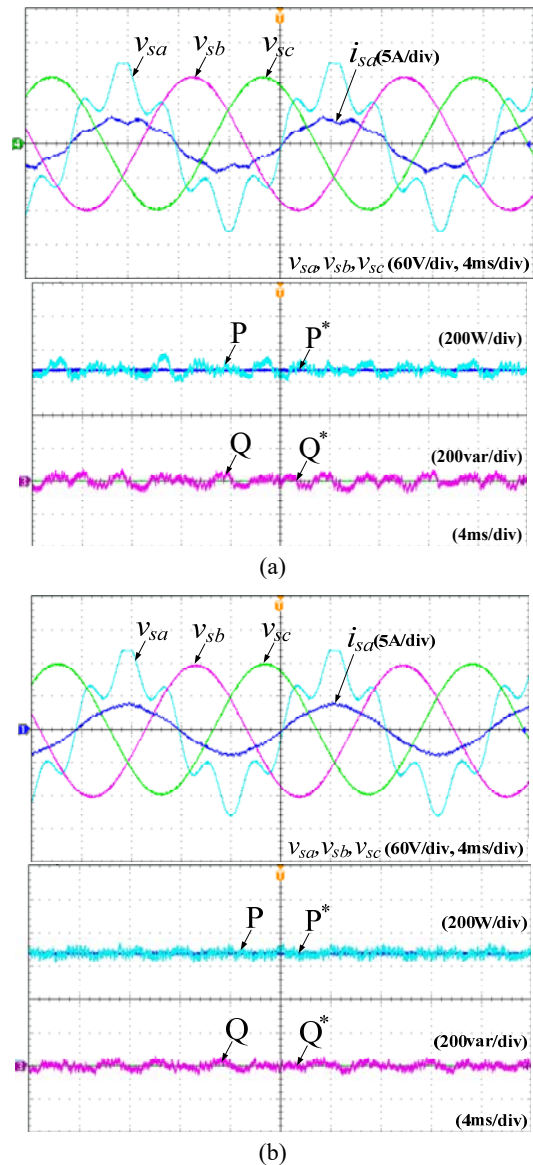

Fig. 9. Experimental results of the three-phase source voltages, the *a*-phase input current, the actual and the reference values of the real and reactive power in case that the *a*-phase source voltage contains the 5th harmonic component by 30% of the fundamental component (a) without the Kalman filter (b) proposed method based on the Kalman filter algorithm.

source voltage without a Kalman filter in Fig. 9 (a). On the other hand, the proposed method based on a Kalman filter can lead to an improved input current waveform due to the filtering effect of the Kalman filter as shown in Fig. 9 (b) when compared with Fig. 9 (a). The frequency spectra of the a-phase input currents are shown in Fig. 10. It can be observed that the total harmonic value of the proposed method is much lower than that of the conventional method under source voltage disturbances.

Experimental results for the dynamic performance of the proposed method with a source voltage disturbance are shown in Fig. 11, with a step-change in the real power
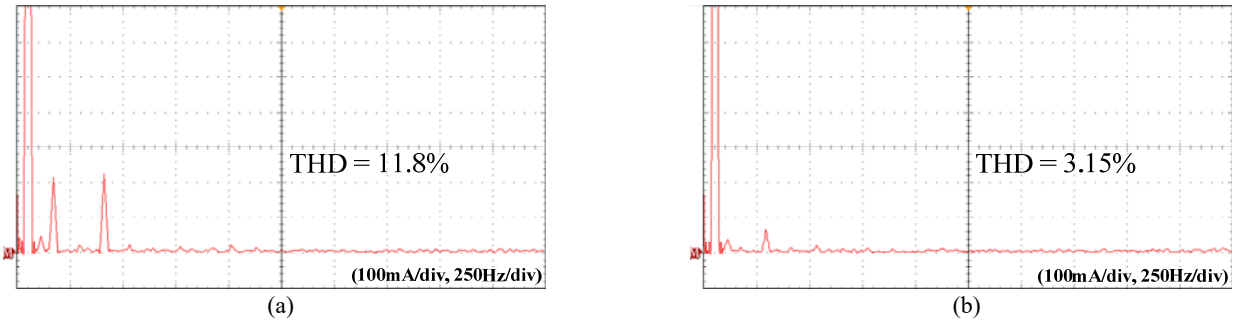
Fig. 10. Frequency spectrum and THD value of the *a*-phase input current (i_{sa}) (a) without the Kalman filter (b) proposed method based on the Kalman filter algorithm.
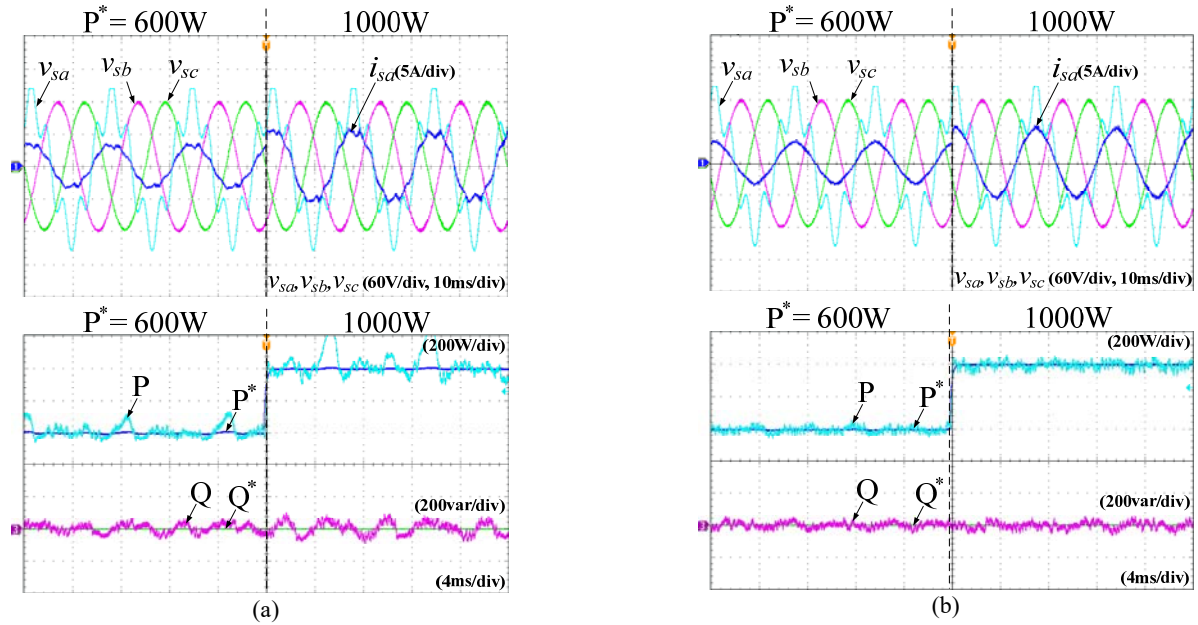

Fig. 11. Experimental results with the step-change of the real power reference from 600 W to 1000 W in the case of *a*-phase source voltage disturbance (a) without the Kalman filter and (b) the proposed method.

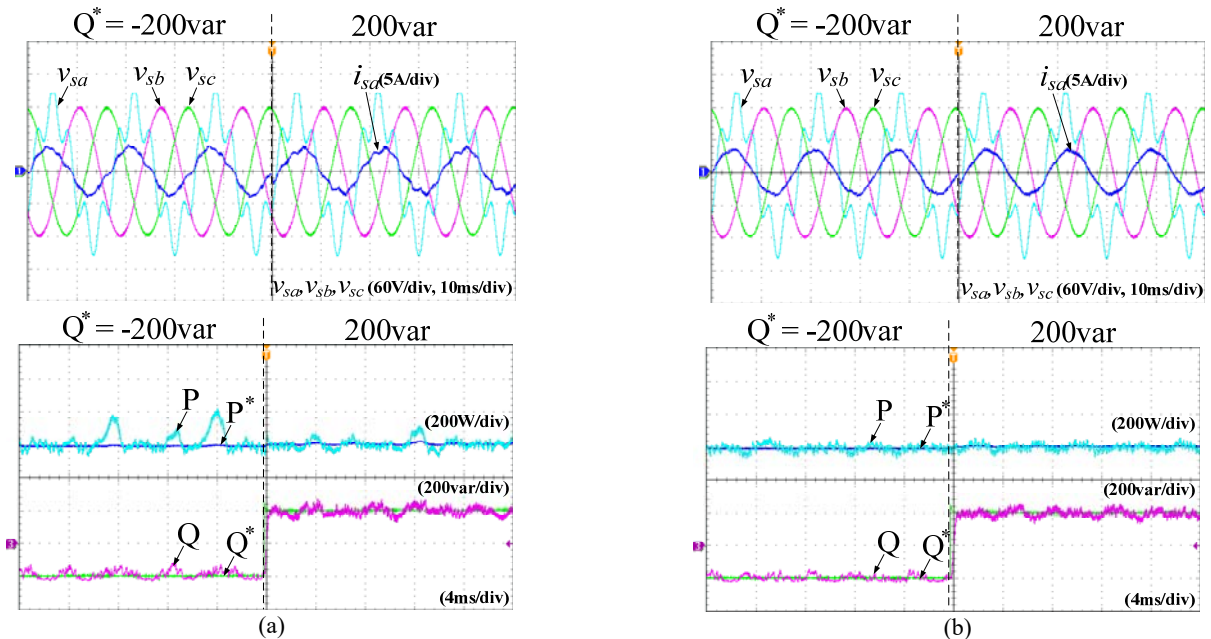Fig. 12. Experimental results with the step-change of the reactive power reference from -200 var to 200 var in the case of *a*-phase source voltage disturbance (a) without the Kalman filter and (b) the proposed method.

reference from 600 W to 1000 W and with the reactive power set to zero. As shown in the Fig. 11, a fast dynamic response and no coupling between the real and reactive power components are obtained by the proposed method. The input current waveform from the proposed method is a sinusoidal waveform with a low THD value in the transient condition with a distorted source voltage as shown in Fig. 11 (b). This is very different from the input current waveform obtained without a Kalman filter in Fig. 11 (a). In addition, simulation results with a step-change in the reactive power reference from -200 var to 200 var, while the real power is fixed to 600 W, are shown in the Fig. 12. It can be seen from Fig. 12 (a) that the distorted input current waveform without a Kalman filter results from a distorted source voltage. Like the step-change in the real power reference, the proposed method leads to no coupling between the real and reactive power components and a fast dynamic response according to the step-change of the reactive power reference with the distorted source voltage as shown in the Fig. 12 (b). Furthermore, the proposed method synthesizes a sinusoidal input current despite the distorted source voltage waveform, while the phase difference between the source voltage and the input currents changes depending on the change of the reactive power reference.

V. CONCLUSIONS

A predictive direct power control method based on a Kalman filter is presented for three-phase pulse width modulation (PWM) rectifiers to improve the performance of rectifiers with source voltages distorted with harmonic components. This method can eliminate the harmonic components of source voltage on the basis of the Kalman filter algorithm. In the process of predicting the future real and reactive power to select an optimal voltage vector in the predictive direct power control method, the proposed method utilizes source voltages filtered by a Kalman filter, which can mitigate the adverse effects of distorted source voltages on the control performance. As a result, the quality of the source currents synthesized by PWM rectifiers are improved with a reduced total harmonic distortion value (THD), even under distorted source voltages.

REFERENCES

[1] J. R. Rodriguez, J. W. Dixon, J. R. Espinoza, J. Pontt and J. Lezana, "PWM regenerative rectifiers: State of the art," *IEEE Trans. Ind. Electron.*, Vol. 52, No. I, pp. 5-22, Feb. 2005.

[2] M. P. Kazmierkowski, R. Krishnan, and F. Blaabjerg, *Control in Power Electronics*. New York, NY, USA: Academic, 2002.

[3] N. Mohan, T. M. Underland, and W. P. Robbins, *Power Electronics*, 2nd ed. Hoboken, NJ, USA: Wiley, 1995.

[4] R. Vargas, U. Ammann, and J. Rodriguez, "A generalized class of stationary frame-current controllers for grid-connected ac dc converters," *IEEE Trans. Power Del.*, Vol. 25, No. 4, pp. 2742-2751, Oct. 2010.

[5] S. Kwak and H. A. Toliyat, "Design and rating comparisons of PWM voltage source rectifiers and active power filters for AC drives with unity power factor," *IEEE Trans. Power Electron.*, Vol. 20, No. 5, pp. 1133-1142, Sep. 2005.

[6] S. Kwak and H. A. Toliyat, "Design and performance comparisons of two multi-drive systems with unity power factor," *IEEE Trans. Power Del.*, Vol. 20, No. 1, pp. 417-426, Jan. 2005.

[7] A. Bouafia, J. P. Gaubert and F. Krim, "Predictive direct power control of three-phase pulse width modulation (PWM) rectifier using space-vector modulation (SVM)," *IEEE Trans. Power Electron.*, Vol. 25, No. 1, pp. 228-236, Jan. 2010.

[8] M. Malinowski, "Sensorless control strategies for three-phase PWM rectifiers," Ph.D. dissertation, Inst. Control Ind. Electron., Warsaw Univ. Technol., Warsaw, Poland, 2001.

[9] M. Malinowski, M. P. Kazmierkowski, and A. M. Trzynadlowski, "A comparative study of control techniques for PWM rectifiers in AC adjustable speed drives," *IEEE Trans. Power Electron.*, Vol. 18, No. 6, pp. 1390-1396, Nov. 2003.

[10] M. P. Kazmierkowski and L. Malesani, "Current control techniques for three-phase voltage-source PWM converters: A survey," *IEEE Trans. Ind. Electron.*, Vol. 45, No. 5, pp. 691-703, Oct. 1998.

[11] M. Liserre, A. DellAquila and F. Blaabjerg, "Genetic algorithm-based design of the active damping for an LCL-filter three-phase active rectifier," *IEEE Trans. Power Electron.*, Vol. 19, No. 1, pp. 76-86, Jan. 2004.

[12] B. Yin, R. Oruganti, S. K. Panda, and A. K. S. Bhat, "An output-power control strategy for a three-phase PWM rectifier under unbalanced supply conditions," *IEEE Trans. Ind. Electron.*, Vol. 55, No. 5, pp. 2140-2150, May 2008.

[13] X. H. Wu, S. K. Panda, and J. X. Xu, "DC link voltage and supply side current harmonics minimization of three phase PWM boost rectifiers using frequency domain based repetitive current controllers," *IEEE Trans. Power Electron.*, Vol. 23, No. 4, pp. 1987-1997, Jul. 2008.

[14] S. Kwak and J. Park, "Predictive control method with future zero-sequence voltage to reduce switching losses in three phase voltage source inverters," *IEEE Trans. Power Electron.*, Vol. 30, No. 3, pp. 1558-1566, Mar. 2015.

[15] J. Alonso-Martínez, J. Eloy-García, D. Santos-Martín, and S. Arnalte, "A new variable frequency optimal direct power control algorithm," *IEEE Trans. Ind. Electron.*, vol. 60, no. 4, pp. 1442-1451, Apr. 2013.

[16] M. Malinowksi, M. P. Kazmierkowski, S. Hansen, F. Blaabjerg, and G. Marques, "Virtual-flux-based direct power control of three-phase PWM rectifiers," *IEEE Trans. Ind. Appl.*, Vol. 37, No. 4, pp. 1019-1027, Jul./Aug. 2001.

[17] Y. Zhang, X. Wu, X. Yuan, Y. Wang and P. Dai, "Fast model predictive control for multilevel cascaded H-Bridge

STATCOM with polynomial computation time," *IEEE Trans. Ind. Electron*., Vol. 63, No. 8, pp. 5231-5243, Aug. 2016.

[18] S. Vazquez, J. Leon, L.G. Franquelo, J. Rodriguez, H. Young, A. Marquez, and P. Zanchetta, "Model predictive control: A review of its applications in power electronics," *IEEE Ind. Electron. Mag*., Vol. 8, No.1, pp. 16-31, Mar. 2014.

[19] S. Kwak and J. C. Park, "Model-predictive direct power control with vector preselection technique for highly efficient active rectifiers," *IEEE Trans. Ind. Informat.*, Vol. 11, No. 1, pp. 44-52, Feb. 2015.

[20] S. Kouro, M. A. Perez, J. Rodriguez, A. M. Llor, and H. A. Young, "Model predictive control: MPC's role in the evolution of power electronics," *IEEE Ind. Electron. Mag.*, Vol. 9, No. 4, pp. 8-21, 2015.

[21] D. E. Catlin, Estimation, *Control and the Discrete Kalman*

[22] *Filter*, Springer-Verlag, 1989.

Un-chul Moon received his B.S., M.S., and Ph.D. degrees from Seoul National University, Seoul, Korea, in 1991, 1993, and 1996, respectively, all in Electrical Engineering. From 1996 to 2000, he was with Samsung, Korea. Since 2000, he has been with Wooseok University, Jeonju, Korea, and Chung-ang University, Seoul, Korea, where he is presently working as a Professor of Electrical and Electronics Engineering. His current research interests include power system analysis, automation, and intelligence systems applied to power systems and power electronics.

Soo-eon Kim received his B.S. degree in Electrical and Electronics Engineering from Chung-ang University, Seoul, Korea, in 2014, where he is presently working towards his M.S. degree in Electrical and Electronics Engineering. His current research interests include the analysis and control of voltage source inverters and active front ends.

Roh Chan received his B.S. degree in Railroad Electrical and Electronics Engineering from the Korea National University of Transportation, Uiwang, Korea, in 2015. Since 2015, he has been working towards his combined M.S. and Ph.D. degrees in Electrical and Electronics Engineering at Chung-ang University, Seoul, Korea. His current research interests include the analysis and control of voltage source inverters and multi-level inverters.

Sangshin Kwak (S'02-M'05) received his Ph.D. degree in Electrical Engineering from Texas A&M University, College Station, TX, USA, in 2005. From 1999 to 2000, he worked as a Research Engineer at LG Electronics, Changwon, Korea. In 2004, he was with the Whirlpool R&D Center, Benton Harbor, MI, USA. From 2005 to 2007, he worked as a Senior Engineer in the Samsung SDI R&D Center, Yongin, Korea. From 2007 to 2010, he worked as an Assistant Professor at Daegu University, Gyeongsan, Korea. Since 2010, he has been at Chung-ang University, Seoul, Korea, where he is presently working as an Associate Professor. His current research interests include the topology design, modeling, control, and analysis of ac/dc, dc/ac, ac/ac power converters including resonant converters for adjustable speed drives and digital display drivers, as well as modern control theory applied to DSP-based power electronics.